

An Examination of the Cloud Curves of Liquid–Liquid Immiscibility in Aqueous Solutions of Alkyl Polyoxyethylene Surfactants Using the SAFT-HS Approach with Transferable Parameters

M. Nieves García-Lisbona,[†] Amparo Galindo,[†] George Jackson,^{*,‡} and Andrew N. Burgess[‡]

Contribution from the Department of Chemistry, University of Sheffield, Sheffield S3 7HF, U.K., and Research and Technology, ICI, P.O. Box 8, The Heath, Runcorn, Cheshire WA7 4QD, U.K.

Received October 21, 1997. Revised Manuscript Received January 28, 1998

Abstract: The phase equilibria of aqueous solutions of *n*-alkyl polyoxyethylene ethers (C_{*i*}E_{*j*}) are characterized by the presence of so-called cloud curves which represent the region of liquid–liquid immiscibility of two micellar solutions (one rich and one poor in surfactant). The systems exhibit a lower critical solution temperature (LCST), which denotes the lower limit of immiscibility; in some cases a complete closed-loop region with an upper critical solution temperature (UCST) is seen corresponding to re-entrant miscibility. In this case the behavior can be explained in terms of the competition between the incompatibility of water with the alkyl chain and the hydrogen bonding between water and the head groups. We have used a simplified version of the statistical associating fluid theory (SAFT), which is based on the thermodynamic perturbation theory of Wertheim for associating fluids: the original SAFT-LJ equation of state treats the molecules as chains of Lennard-Jones segments while the simplified SAFT-HS equation treats molecules as chains of hard-sphere repulsive segments with van der Waals interactions. The water molecules are modeled as hard spheres with four associating sites to treat the hydrogen bonding; the dispersion forces are treated at the van der Waals mean-field level. The surfactant molecules are modeled as chains of hard-sphere segments with two or three bonding sites to treat the terminal hydroxyl group and an additional three sites per oxyethylene group; the dispersion forces are again treated at the mean-field level. For appropriate choices of the intermolecular parameters, the SAFT-HS approach predicts cloud curves with both a UCST and an LCST. The critical temperatures and the extent of immiscibility are in very good agreement with the experimental data. We have studied the transferability of the intermolecular potential parameters for different members of the C_{*i*}E_{*j*} homologous series. Although the general trends are reproduced, slightly different values of the unlike dispersion forces have to be used for the various systems in order to provide quantitative agreement with experiment. This is not altogether surprising for such complex aqueous micellar solutions. We have explored a relationship between the structure of the surfactant molecule and the value of the unlike intermolecular potential parameter which enables one to predict the phase behavior of aqueous solutions of any member of the C_{*i*}E_{*j*} homologous series.

Introduction

Alkyl polyoxyethylene ethers constitute a family of substances which behave as surface active agents in aqueous solutions. These compounds are represented by the general chemical structure H(CH₂)_{*i*}(OCH₂CH₂)_{*j*}OH, or simply C_{*i*}E_{*j*}, where *i* refers to the number of carbon atoms in the alkyl residue and *j* to the number of oxyethylene (–OCH₂CH₂–) units in the molecule; the molecules also possess a terminal hydroxyl (–OH) group. Each oxyethylene unit is only weakly polar so a relatively large number of *j* units is necessary to confer surfactant properties on the molecules. These molecules are very malleable, since their hydrophobic and hydrophilic characteristics can easily be manipulated by changing *i* and/or *j*. Alkyl polyoxyethylene surfactants have numerous applications in areas as diverse as oil recovery, cosmetics, detergents, or refrigerants.

The study of surfactants and their behavior in solution plays an important role in industrial applications. The large number of processes which occur in solution justifies the need for effective and, in many cases, mild surfactants. Researchers will

always be looking for new, better surfactant mixtures, notwithstanding their own scientific curiosity for the remarkable properties of these systems. Mixtures containing surfactants display very interesting types of phase behavior, with features such as micelle formation, liquid–liquid immiscibility, or the presence of liquid crystalline structures.

Aqueous solutions of alkyl polyoxyethylene ethers are no exception. These systems have been extensively studied, and phenomena of the type mentioned above have been reported in the literature.^{1–20} One of the main features in the phase diagram of aqueous solutions of these compounds is the presence of

- (1) Chakhovskoy, N. *Bull. Soc. Chim. Belg.* **1956**, *65*, 474–493.
- (2) Mulley, B. A.; Metcalf, A. D. *J. Colloid Sci.* **1964**, *19*, 501–515.
- (3) Clunie, J. S.; Corkill, J. M.; Goodman, J. F.; Symons, P. C.; Tate, J. R. *Trans. Faraday Soc.* **1967**, *63*, 2839–2845.
- (4) Marland, J. S.; Mulley, B. A. *J. Pharm. Pharmacol.* **1971**, *23*, 561–572.
- (5) Harusawa, F.; Nakamura, S.; Mitsui, T. *Colloid Polym. Sci.* **1974**, *252*, 613–619.
- (6) Ali, A. A.; Mulley, B. A. *J. Pharm. Pharmacol.* **1978**, *30*, 205–213.
- (7) Lang, J. C.; Morgan, R. D. *J. Chem. Phys.* **1980**, *73*, 5849–5861.
- (8) Corti, M.; Degiorgio, V. *Phys. Rev. Lett.* **1980**, *45*, 1045–1048.

[†] University of Sheffield.

[‡] ICI.

liquid–liquid immiscibility. With increasing temperature an initially homogeneous mixture becomes immiscible above a lower critical solution temperature (LCST), resulting in a system in which two phases, one rich in water and the other rich in surfactant, coexist. The immiscibility can persist at higher temperatures or, in many cases, disappear above a second critical point, the upper critical solution temperature (UCST), resulting in what is known as a closed-loop coexisting curve. The LCST region for a wide number of aqueous solutions of alkyl polyoxyethylene surfactants has been studied in the papers of Mitchell *et al.*,⁹ Corti *et al.*,¹⁰ and Schubert *et al.*¹⁷ Most of these systems would very likely show closed-loop immiscibility if they were investigated at sufficiently high temperatures, but due to the temperature instability of the molecules only the LCST region has been examined. It should be noted that, in general, when considering the LCST region and referring to surfactant molecules in solution, one is in fact studying complex entities, i.e., surfactant micelles, since the critical micelle concentration (CMC) curves for these systems are at lower concentrations than the miscibility gaps. To our knowledge, the only two systems for which the region of UCST coexistence has been examined appear in the paper of Lang and Morgan,⁷ a landmark in the study of aqueous solutions of alkyl polyoxyethylene surfactants. They studied the cloud curves for C₁₀E₄ and C₁₀E₅ in aqueous solutions and determined the regions of stability of the various liquid crystalline phases. Aqueous solutions of alkyl polyoxyethylene surfactants are typical lyotropic liquid crystalline systems which display cubic, hexagonal, and lamellar structures formed by the micellar aggregates.²¹ The phase behavior of these systems also exhibits large regions of liquid–liquid immiscibility between two micellar solutions which are bound above and below by a UCST and an LCST, respectively. In the case of the C₁₀E₄ system the liquid–liquid equilibria are complicated by the intrusion of the liquid crystalline phases at lower temperatures. However, in the case of the C₁₀E₅ system a well-defined closed-loop coexistence curve is seen: the UCST appears at $T = 567$ K and 31% (by weight) surfactant and the LCST at $T = 317$ K and 5%, respectively; the width of the coexistence curve extends to about 80%. The closed loops are very asymmetric; the lower critical compositions are displaced relatively to the upper critical compositions, a distinctive feature which is difficult to reproduce by any of the theoretical treatments which have dealt with this type of system. In this paper we focus on a theoretical prediction of the liquid–liquid coexistence, leaving a study of

liquid crystalline phases and micellization also exhibited by the systems for future work.

The phenomenon of closed-loop immiscibility can be explained in terms of a competition between energetic and entropic contributions to the free energy of the system. In order to minimize its free energy, a system will try to adopt the most favorable conformation at each temperature. At high temperatures this will result in a homogeneous mixture, since the system maximizes its compositional and orientational entropy, the dominant effects. As the temperature is decreased, the enthalpic contribution becomes dominant in the free energy balance; unfavorable van der Waals forces between unlike molecules provoke phase separation, and liquid–liquid immiscibility occurs. If the temperature is lowered further, the enthalpic contribution due to hydrogen bonding between unlike species overcomes any other unfavorable effects and the system becomes once more completely miscible (a more detailed introduction to this type of behavior can be found in ref 22).

The theoretical prediction of the phenomenon of closed-loop immiscibility has been of long-standing interest (see refs 23 and 24 for an overview), and will not be reviewed here. It is, however, important to mention the work of Hirschfelder and co-workers,²⁵ who were the first to suggest directional attractive forces such as hydrogen bonding as the direct cause of the appearance of an LCST.

Other theoretical studies of closed-loop immiscibility have focused on the phase behavior of aqueous solutions of alkyl polyoxyethylene surfactants. Of particular interest are several studies which adopt a phenomenological approach^{26–30} to describe closed-loop immiscibility for the type of mixtures of interest here. Angle-averaged intermolecular pair potentials are used to represent systems with highly anisotropic interactions. These pair potentials must be strongly temperature dependent in order to give rise to re-entrant solubility, caused by the thermal disruption of hydrogen bonds. Goldstein^{26,27} addressed the problem by defining a partition function which included van der Waals and hydrogen bonding contributions, combined with the Flory–Huggins free energy. Micellar solutions of nonionic surfactants were studied,²⁸ and qualitative agreement with the experimental closed-loop phase behavior was found. Following a similar continuum approach, Reatto and Tau²⁹ studied mixtures of spherical molecules with long-range attractive interactions. They used a temperature-dependent potential of mean force to incorporate solvent effects into the model. The size of the spheres was made to decrease as the temperature was increased, to justify the decreasing size of the hydration shell. Evans and co-workers³⁰ extended this study to examine the LCSTs exhibited by a number of aqueous solutions of alkyl polyoxyethylene ethers using a perturbation theory. Good agreement with experimental data was achieved, though often at the expense of unreasonable physical assumptions in the model. Phenomenological approaches all suffer from a fundamental problem: since the exact form of the temperature-dependent interactions for hydrogen-bonded systems is un-

(9) Mitchell, D. J.; Tiddy, G. J. T.; Waring, L.; Bostock, T.; McDonald, M. P. *J. Chem. Soc., Faraday Trans.* **1983**, *19*, 975–1000.

(10) Corti, M.; Minero, C.; Degiorgio, V. *J. Phys. Chem.* **1984**, *88*, 309–317.

(11) Cantù, L.; Corti, M.; Degiorgio, V.; Minero, C.; Piazza, R. *J. Colloid Interface Sci.* **1985**, *105*, 628–634.

(12) de Salvo Souza, L.; Corti, M.; Cantù, L.; Degiorgio, V. *Chem. Phys. Lett.* **1986**, *131*, 160–164.

(13) Carvell, M.; Leng, C. A.; Leng, F. J.; Tiddy, G. J. T. *Chem. Phys. Lett.* **1987**, *137*, 188–190.

(14) Kahlweit, M.; Strey, R.; Firman, P.; Haase, D.; Jen, J.; Schomäcker, R. *Langmuir* **1988**, *4*, 499–511.

(15) Andersson, B.; Olofsson, G. *J. Solution Chem.* **1989**, *18*, 1019–1035.

(16) Strey, R.; Schomäcker, R.; Roux, D.; Nallet, F.; Olsson, U. *J. Chem. Soc., Faraday Trans.* **1990**, *86*, 2253–2261.

(17) Schubert, K.-V.; Strey, R.; Kahlweit, M. *J. Colloid Interface Sci.* **1991**, *141*, 21–29.

(18) Puvvada, S.; Blankschtein, D. *J. Phys. Chem.* **1992**, *96*, 5579–5592.

(19) Sassen, C. L.; Gonzalez Casielles, A.; de Loos, Th. W.; de Swaan Arons, J. *Fluid Phase Equilib.* **1992**, *72*, 173–187.

(20) Lim, K.-H.; Reckley, J. S.; Smith, D. H. *J. Colloid Interface Sci.* **1993**, *161*, 465–470.

(21) Tiddy, G. J. T. *Phys. Rep.* **1980**, *57*, 1–46.

(22) Walker, J. S.; Vause, C. A. *Sci. Am.* **1987**, *256*, 90–97.

(23) Jackson, G. *Mol. Phys.* **1991**, *72*, 1365–1385.

(24) García-Lisbona, M. N.; Galindo, A.; Jackson, G.; Burgess, A. N. *Mol. Phys.* **1998**, *93*, 57–71.

(25) Hirschfelder, J.; Stevenson, D.; Eyring, H. *J. Chem. Phys.* **1937**, *5*, 896–912.

(26) Goldstein, R. E. *J. Chem. Phys.* **1984**, *80*, 5340–5341.

(27) Goldstein, R. E. *J. Chem. Phys.* **1985**, *83*, 1246–1254.

(28) Goldstein, R. E. *J. Chem. Phys.* **1986**, *84*, 3367–3378.

(29) Reatto, L.; Tau, M. *Chem. Phys. Lett.* **1984**, *108*, 292–296.

(30) Evans, H.; Tildesley, D. J.; Leng, C. A. *J. Chem. Soc., Faraday Trans. 2* **1987**, *83*, 1525–1541.

known, only qualitative assumptions about the potential can be made, and these can be quite unphysical.

Knudsen and co-workers³¹ have used UNIQUAC–UNIFAC models, combined with the Soave–Redlich–Kwong equation of state,³² to study aqueous solutions of *n*-butoxyethanol (C_4E_1). This type of semiempirical model, based on the activity coefficient, achieves reasonable agreement with experimental data, despite the fact that it does not explicitly account for anisotropic interactions and that a large number of interaction parameters have to be used.

In contrast to phenomenological and activity coefficient approaches, we choose a potential which incorporates the directional nature of the hydrogen bond, and therefore can be used to predict re-entrant miscibility at low temperatures. We use a simplified version of the statistical associating fluid theory (SAFT) which in its original formalism treats molecules as chains of Lennard-Jones segments.^{33–36} The version used here, SAFT-HS, describes molecules as chains of hard-sphere segments with associating bonding sites to model hydrogen bonding, and long-range dispersion forces are treated at the van der Waals mean-field level. The use of the simplest version of the theory is justified in systems where there is strong association so that the dispersion forces can be treated at the mean-field level. The SAFT-HS formalism has already been used to describe closed-loop immiscibility in associating model mixtures of spherical and chain molecules.^{23,37} In a more recent paper,²⁴ we have used SAFT-HS to study the phase equilibria of aqueous systems containing 1-butanol (C_4E_0) and two alkyl polyoxyethylene ethers (C_4E_1 and $C_{10}E_5$), where closed-loop liquid–liquid immiscibility is a major feature of the phase behavior. In the present work we extend the study to aqueous mixtures of the entire alkyl polyoxyethylene ether homologous series using information obtained in our previous study.²⁴ The goal of our work is 2-fold: on the one hand, we aim to achieve quantitative agreement with experimental LCST data; on the other, we want to use the SAFT-HS formalism in a transferable manner within the homologous series, a feature that would improve the predictive capability of our treatment. In practical terms this means that we aim to use a unique set of intermolecular parameters which can be used to describe the phase equilibria of any member of the homologous series and its mixture with water.

Models and Theory

In the modeling and theoretical treatment of aqueous solutions of alkyl polyoxyethylene surfactants we follow the approach of our previous work,²⁴ which we will refer to as paper I. Only the central points of the molecular models and the theory used in paper I will therefore be included here, mainly for the purpose of completeness. The reader is directed to the original paper or to the authors for further detail.

The water molecule (component 1) is modeled as a hard sphere of diameter σ_1 with four off-center square-well attractive sites that mediate intermolecular association (see Figure 1a));

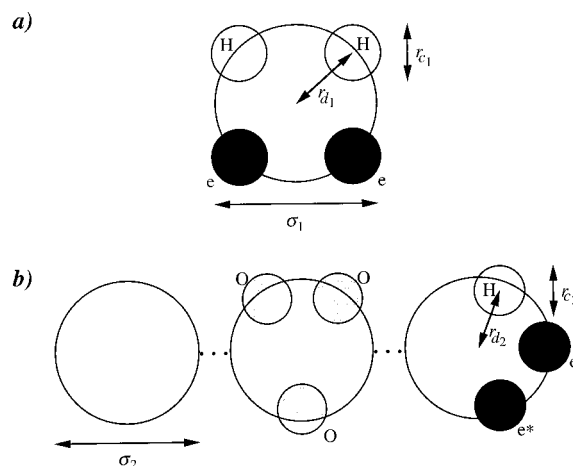


Figure 1. Models for (a) H_2O and (b) C_iE_j (alkyl polyoxyethylene series). The molecules are modeled as hard spheres or chains of hard spheres of diameter σ_k with a number of off-center square-well bonding sites. The sites are at a distance r_{dk} from the center of the sphere and have a range r_{ek} . Water is modeled as a single hard sphere with four bonding sites: two of type e and two of type H. Only H–e bonding is allowed with an energy of ϵ_{11}^{hb} . On the C_iE_j molecules, three sites mediate the unlike hydrogen bond interactions between water and the hydroxyl group (two sites are of type e, and one of type H). Three sites of type O (per oxyethylene unit) hydrogen bond to the H water sites. Only one H site and one e site hydrogen bond in the pure C_iE_j fluid (see the text) with an energy of ϵ_{27}^{hb} . Water and surfactant interact with hydrogen bonding energies of ϵ_{12}^{hb} (water and hydroxyl group) and ϵ_{O12}^{hb} (water and ether group) when the site–site distance is less than r_{ek} . The number of spherical segments building up a C_iE_j molecule is obtained from the simple relation $m_2 = [(C + O + 1)/3 + 1.2]$. Mean-field dispersive interactions are included per spherical segment with integrated energies of ϵ_{11} , ϵ_{22} , and ϵ_{12} .

weak dispersion forces are included at the mean-field level of van der Waals with an integrated energy of ϵ_1 . Two of the sites represent the hydrogens (H) in water and the other two the lone pairs of electrons of the oxygen (e). The sites of the water molecule can be viewed as being placed in a tetrahedral arrangement on the central sphere, although their relative positions are not important at this level of approximation. They are placed at a distance r_{d1} from the center of the sphere, and have a cut-off range r_{e1} ; these two parameters define the volume K_1 available for the site–site hydrogen-bond association.³⁸ Two sites, H and e, interact with a hydrogen bonding energy ϵ_{11}^{hb} when they are a distance of less than r_{e1} apart, and no H–H or e–e interaction is allowed.

The alkyl polyoxyethylene surfactants (component 2) are modeled as associating chain molecules with a number m_2 of hard-sphere segments of diameter σ_2 , which account for the nonspherical shape of the molecules, and attractive sites are included to allow for hydrogen bonding (see Figure 1b)); the long-range dispersion forces are included at the mean-field level of van der Waals per spherical segment. The number of spheres m_2 building up a molecule is obtained from the empirical relation given in paper I, $m_2 = [(C + O - 1)/3 + 1] + 0.2$, where C and O are the number of carbon atoms and ether oxygens in the backbone of the molecule and where the term 0.2 accounts for the hydroxyl group. Basically, we have assumed that the ether oxygens contribute to m_2 in the same way as the carbon atoms with respect to the overall molecular length. Note that all segments in the chain are of the same size. Three attractive

(31) Knudsen, K.; Stenby, E. H.; Andersen, J. G. *Fluid Phase Equilib.* **1994**, *93*, 55–74.

(32) Soave, G. *Chem. Eng. Sci.* **1972**, *27*, 1197–1203.

(33) Chapman, W. G.; Gubbins, K. E.; Jackson, G.; Radosz, M. *Fluid Phase Equilib.* **1989**, *52*, 31–38.

(34) Chapman, W. G.; Gubbins, K. E.; Jackson, G.; Radosz, M. *Ind. Eng. Chem. Res.* **1990**, *29*, 1709–1721.

(35) Huang, S. H.; Radosz, M. *Ind. Eng. Chem. Res.* **1990**, *29*, 2284–2294.

(36) Huang, S. H.; Radosz, M. *Ind. Eng. Chem. Res.* **1991**, *30*, 1994–2005.

(37) Green, D. G.; Jackson, G. *J. Chem. Phys.* **1992**, *97*, 8672–8690.

(38) Jackson, G.; Chapman, W. G.; Gubbins, K. E. *Mol. Phys.* **1988**, *65*, 1–31.

sites (one of type H and two of type e) are used to represent the hydroxyl group of the alkyl polyoxyethylene molecules. The H and e sites of the hydroxyl group interact with an energy of ϵ_2^{hb} and a bonding volume of K_2 . In the case of hydrogen bonding between the hydroxyl groups of the surfactant molecules only one of the e sites is active, so that two bonds per hydroxyl group are possible; this reduction in the bonding can be understood in terms of steric hindrance of the molecular tails. We also assume that the steric hindrance will be too large for surfactant–surfactant interaction to occur between the hydroxyl and ether groups down the chain.

All three sites are active in mediating the unlike hydrogen bonding between the hydroxyl group of the surfactants and the water molecules; the corresponding energy and bonding volume are $\epsilon_{12}^{\text{hb}}$ and K_{12} ; basically, this model for the surfactant molecules accounts for the hydration shell of water molecules around the terminal hydroxyl group. The water molecules are also allowed to hydrate (associate with) the ether oxygens along the surfactant chain. For this purpose three additional attractive sites per oxyethylene group are included in the C_iE_j molecule when water is present. The number of sites used to model the interaction between water and the ether oxygens is that which gives the best description of the phase equilibria of the water + surfactant mixtures, taking *n*-butoxyethanol as the prototype C_iE_j molecule (see paper I). We label these sites as type O, and allow them to interact only with the water H sites, resulting in an energy of $\epsilon_{012}^{\text{hb}}$ and a bonding volume of K_{012} .

The actual values of intermolecular potential parameters are obtained from the vapor–liquid equilibria of the pure fluids and from the phase behavior of the mixture; these will be given in the following section. First we will summarize the SAFT-HS formalism for such mixtures. As we have mentioned before, we borrow heavily from paper I and only the central equations will be presented here.

The Helmholtz free energy *A* for an *n*-component mixture of associating chain molecules is separated into different contributions as

$$\frac{A}{NkT} = \frac{A^{\text{IDEAL}}}{NkT} + \frac{A^{\text{MONO}}}{NkT} + \frac{A^{\text{CHAIN}}}{NkT} + \frac{A^{\text{ASSOC}}}{NkT} \quad (1)$$

where *N* is the number of molecules, *T* is the temperature, and *k* is the Boltzmann constant. The precise form of the ideal contribution to the free energy A^{IDEAL} can be found in paper I, and is given by the usual ideal mixture expressions.³⁹ The monomer–monomer contribution A^{MONO} to the free energy in the mixture consists of a sum of two contributions: a repulsive term A^{HS} for a mixture of hard spheres, given by the expressions of Boublík⁴⁰ and Mansoori *et al.*,⁴¹ and an attractive contribution A^{MF} from the long-range dispersion forces, given at the mean-field level in terms of the van der Waals one-fluid theory.⁴² The contribution to the free energy due to chain formation A^{CHAIN} , the other repulsive contribution to the equation of state, is taken from the work of Chapman *et al.*⁴³ The contribution due to association A^{ASSOC} is obtained from the theory of Wertheim (see ref 43). For the model $\text{H}_2\text{O} + C_iE_j$ mixtures of

(39) Hansen, J. P.; McDonald, I. N. *Theory of Simple Liquids*, 2nd ed.; Academic Press: London, 1986.

(40) Boublík, T. *J. Chem. Phys.* **1970**, *53*, 471–472.

(41) Mansoori, G. A.; Carnahan, N. F.; Starling, K. E.; Leland, T. W. *J. Chem. Phys.* **1971**, *54*, 1523–1525.

(42) Rowlinson, J. S.; Swinton, F. L. *Liquids and Liquid Mixtures*, 3rd ed.; Butterworth Scientific: London, 1982.

(43) Chapman, W. G.; Jackson, G.; Gubbins, K. E. *Mol. Phys.* **1988**, *65*, 1057–1079.

interest here the expression for A^{ASSOC} takes the form of

$$\begin{aligned} \frac{A^{\text{ASSOC}}}{NkT} = & x_1 \left[2 \left(\ln X_{\text{H1}} - \frac{X_{\text{H1}}}{2} \right) + 2 \left(\ln X_{\text{e1}} - \frac{X_{\text{e1}}}{2} \right) + \frac{4}{2} \right] + \\ & x_2 \left[\left(\ln X_{\text{H2}} - \frac{X_{\text{H2}}}{2} \right) + \left(\ln X_{\text{e2}} - \frac{X_{\text{e2}}}{2} \right) + \left(\ln X_{\text{e2}^*} - \frac{X_{\text{e2}^*}}{2} \right) + \right. \\ & \left. 3j \left(\ln X_{\text{O2}} - \frac{X_{\text{O2}}}{2} \right) + \frac{(3j+3)}{2} \right] \quad (2) \end{aligned}$$

where x_k is the mole fraction of component *k*, *j* is the number of oxyethylene groups in the surfactant molecule, X_{H1} and X_{e1} are the fraction of water molecules not bonded at sites H and e, and X_{H2} , X_{e2} , X_{e2^*} , and X_{O2} are the fraction of surfactant molecules not bonded at sites H, e, e*, and O.

The general equation for the fraction of free molecules of a given type *k* not bonded at a site *a*, $X_{a,k}$, is obtained from a self-consistent iterative solution⁴⁴ of the mass action equation:⁴³

$$X_{a,k} = \frac{1}{1 + \sum_{l=1} \sum_{b=1} \rho x_l X_{b,l} \Delta_{a,b,k,l}} \quad (3)$$

$x_l = N_l/N$ is the mole fraction of component *l*, $\rho = N/V$ the total number density, *N* the number of molecules, and *V* the volume of the system. The function $\Delta_{a,b,k,l}$ characterizes the association between site *a* on a molecule of species *k* and site *b* on a molecule of species *l*, and will be different for each type of site–site interaction (see paper I). It can be written in terms of the contact value $g^{\text{HS}}(\sigma_{kl})$ of the radial distribution function of the reference segment–segment hard-sphere interaction, the Mayer *f* function $F_{a,b,k,l} = \exp(\epsilon_{a,b,k,l}^{\text{hb}}/kT) - 1$ of the square-well *a*–*b* site–site bonding interaction $\epsilon_{a,b,k,l}^{\text{hb}}$ and the volume $K_{a,b,k,l}$ available for bonding.⁴³

$$\Delta_{a,b,k,l} = K_{a,b,k,l} F_{a,b,k,l} g^{\text{HS}}(\sigma_{kl}) \quad (4)$$

We use Boublík's⁴⁰ expression for the pair distribution function at contact σ_{kl} . The extent of association depends on the strength of the interaction through *F* and on the position and range of the site–site interaction through *K*. The precise details of the position and range of the sites are not important at this level of approximation as long as they correspond to the same integrated bonding volume *K*.

For the $\text{H}_2\text{O} + C_iE_j$ mixtures, the fractions of molecules not bonded at given sites are obtained from eq 3 as

$$X_{\text{H1}} = \frac{1}{1 + 2\rho x_1 X_{\text{e1}} \Delta_{11} + \rho x_2 X_{\text{e2}} \Delta_{12} + \rho x_2 X_{\text{e2}^*} \Delta_{12} + 3j\rho x_2 X_{\text{O2}} \Delta_{012}} \quad (5)$$

$$X_{\text{e1}} = \frac{1}{1 + 2\rho x_1 X_{\text{H1}} \Delta_{11} + \rho x_2 X_{\text{H2}} \Delta_{12}} \quad (6)$$

$$X_{\text{H2}} = \frac{1}{1 + 2\rho x_1 X_{\text{e1}} \Delta_{21} + \rho x_2 X_{\text{e2}} \Delta_{22}} \quad (7)$$

(44) Press, W. H.; Flannery, B. P.; Teukolsky, S. A.; Vetterling, W. T. *Numerical Recipes in Fortran*, 1st ed.; Cambridge University Press: Cambridge, 1986.

$$X_{e2} = \frac{1}{1 + 2\rho x_1 X_{H1}\Delta_{21} + \rho x_2 X_{H2}\Delta_{22}} \quad (8)$$

$$X_{e2}^* = \frac{1}{1 + 2\rho x_1 X_{H1}\Delta_{21}} \quad (9)$$

$$X_{O2} = \frac{1}{1 + 2\rho x_1 X_{H1}\Delta_{O21}} \quad (10)$$

Each $\Delta_{a,b,k,l}$ defines a different type of association: Δ_{11} , association between H and e sites of water molecules; Δ_{12} ($\Delta_{21} = \Delta_{12}$), association between water and the hydroxyl group of the surfactant; Δ_{22} , self-association of the hydroxyl groups; and Δ_{O12} ($\Delta_{O21} = \Delta_{O12}$), association between water and the ether oxygens of the surfactant.

In the calculation of the phase equilibria of the mixtures it is useful to use a series of reduced parameters, simply for reasons of convenience. These parameters are defined as follows. The volume of a spherical segment is denoted by $b_k = \pi\sigma_k^3/6$, and the integrated energy of the van der Waals mean-field interaction by $\epsilon_k = \alpha_{kk}/b_k$, where α_{kk} is the corresponding van der Waals attractive constant. All the parameters of the mixture are reduced relative to one of the components, component 1 in our case, so that $\sigma_{kl}^* = \sigma_{kl}/\sigma_1$, $\alpha_{kl}^* = \alpha_{kl}/\alpha_1$, etc. The range and position of the bonding sites are reduced with respect to the diameter of the particular sphere in which they are included, i.e., $r_{c1}^* = r_{c1}/\sigma_1$ and $r_{d1}^* = r_{d1}/\sigma_1$ while $r_{c2}^* = r_{c2}/\sigma_2$ and $r_{d2}^* = r_{d2}/\sigma_2$. The reduced bonding volume for each of the pure components is calculated as⁴³

$$K_k^* = \frac{K_k}{\sigma_k^3} = 4\pi[\ln(r_{c_k}^* + 2r_{d_k}^*)(6r_{c_k}^{*3} + 18r_{c_k}^{*2}r_{d_k}^* - 24r_{d_k}^{*3}) + (r_{c_k}^* + 2r_{d_k}^* - 1)(22r_{d_k}^{*2} - 5r_{c_k}^*r_{d_k}^* - 7r_{d_k}^* - 8r_{c_k}^{*2} + r_{c_k}^* + 1)]/(72r_{d_k}^{*2}) \quad (11)$$

and can then be written in terms of one of the two components. The reduced energy for the site-site interaction is defined in terms of the mean-field interaction of component 1, $\epsilon_k^{\text{hb}*} = \epsilon_k^{\text{hb}}/\epsilon_1$.

Results and Discussion

The intermolecular potential parameters for the pure components and mixtures are obtained from the appropriate experimental phase equilibria. Details of the approach have been given in paper I. The parameters of the intermolecular potential model for water are obtained by fitting the theoretical predictions to experimental vapor-liquid equilibria⁴⁵ using a simplex method.⁴⁴ The optimized size of the spherical hard core is $\sigma_1 = 3.60 \text{ \AA}$, the integrated mean-field energy $\epsilon_1/k = 4452 \text{ K}$, the energy of the site-site hydrogen bonding $\epsilon_1^{\text{hb}}/k = 1558 \text{ K}$, and the bonding volume for the site-site interaction $K_1 = 1.3578 \text{ \AA}^3$ ($r_{c1}^* = 0.679$ and $r_{d1}^* = 0.25$).

In the case of the alkyl polyoxyethylene surfactants, we take advantage of the transferability of parameters of the simple SAFT-HS approach.⁴⁶ Since association is mediated through square-well bonding sites embedded in the hard-sphere cores,

and the contribution to the free energy due to hydrogen bonding is accounted for separately, the backbone chain can be treated as equivalent to an alkyl residue. By adopting this approach, we can use the parameters reported in a previous study of *n*-alkanes⁴⁶ to describe the size of the spherical segments as $\sigma_2 = 3.855 \text{ \AA}$, and the strength of the dispersive interactions as $\epsilon_2/k = 3135 \text{ K}$. The only association we allow between pure polyoxyethylene molecules is through the terminal hydroxyl group. The parameters of the hydrogen bonding between hydroxyl groups are obtained by refitting to the experimental vapor pressure of butoxyethanol (C_4E_1),⁴⁷ resulting in an energy of $\epsilon_2^{\text{hb}}/k = 3448 \text{ K}$ and a bonding volume of $K_2 = 0.391 \text{ \AA}^3$ ($r_{c2}^* = 0.613$ and $r_{d2}^* = 0.25$); the bonding volume is slightly different from that used in paper I, but provides an excellent description of the longer molecules in the C_iE_j homologous series. The actual value of $K_2 = 0.391 \text{ \AA}^3$ corresponds to that obtained for 1-butanol (C_4E_0) (see paper I) by fitting to vapor pressure and saturated liquid density data.⁴⁷ The C_4E_0 molecule can be considered as the first member of the C_4E_j series, and similarly C_4E_1 can be regarded as the first molecule of the C_4E_j series which contains an oxyethylene group.

To recap, the values of the parameters of the intermolecular potential used to model all the members of the C_iE_j series are $\sigma_2 = 3.855 \text{ \AA}$, $\epsilon_2/k = 3135 \text{ K}$, $\epsilon_2^{\text{hb}}/k = 3448 \text{ K}$, and $K_2 = 0.391 \text{ \AA}^3$, and m_2 is obtained from the relation $m_2 = [(C + O + 1)/3 + 1.2]$.

The unlike parameters, which account for the interactions between unlike components in the mixture, are determined from those of the pure components. The geometric mean of the energy parameters of the pure components and the arithmetic mean of the size-related parameters of pure components are generally used. Since our models comprise hard-sphere segments, the unlike size parameter σ_{12} in a mixture is obtained as the arithmetic mean of σ_1 and σ_2 . Similarly, the bonding volume between sites on different molecules can be approximated as

$$K_{12}^* = \frac{K_{12}}{\sigma_1^3} = \left[\frac{(K_1/\sigma_1^3)^{1/3} + (K_2/\sigma_1^3)^{1/3}}{2} \right]^3 \quad (12)$$

The phase behavior of many mixtures cannot, however, be predicted using unlike energies calculated with the geometric mean of the pure component energy parameters. We treat the unlike integrated mean-field energy ϵ_{12} and the site-site energies of the hydrogen bond between unlike molecules $\epsilon_{12}^{\text{hb}}$ (for the water and hydroxyl group) and $\epsilon_{O12}^{\text{hb}}$ (for the water and ether oxygens) as adjustable parameters, and optimize them to give the best representation of the phase equilibria of the mixtures.

The strength of the unlike site-site interaction $\epsilon_{12}^{\text{hb}}$ was determined by fitting to the liquid-liquid phase equilibria of the mixture water + 1-butanol (see paper I). The value of $\epsilon_{12}^{\text{hb}}/k = 1803 \text{ K}$ (which corresponds to a reduced parameter of $\epsilon_{12}^{\text{hb}*} = 0.405$) gives the best overall representation of the high-pressure phase equilibria of this mixture. Since the first member of the C_4E_j series which contains bonding sites of type O is butoxyethanol, the $\epsilon_{O12}^{\text{hb}}$ energy is obtained by fitting to the phase equilibria of the water + butoxyethanol mixture in the region of liquid-liquid immiscibility.⁴⁸ The optimum value of

(45) *Handbook of Chemistry and Physics*, 60th ed.; CRC Press: Boca Raton, FL, 1981.

(46) Galindo, A.; Whitehead, P. J.; Jackson, G.; Burgess, A. N. *J. Phys. Chem.* **1996**, *100*, 6781-6792.

(47) Smith, B. D.; Srivastava, R. *Thermodynamic Data for Pure Compounds*; Elsevier: London, 1986.

(48) Aizpiri, A. G.; Monroy, F.; del Campo, C.; Rubio, R. G.; Díaz Peña, M. *Chem. Phys.* **1992**, *165*, 31-39.

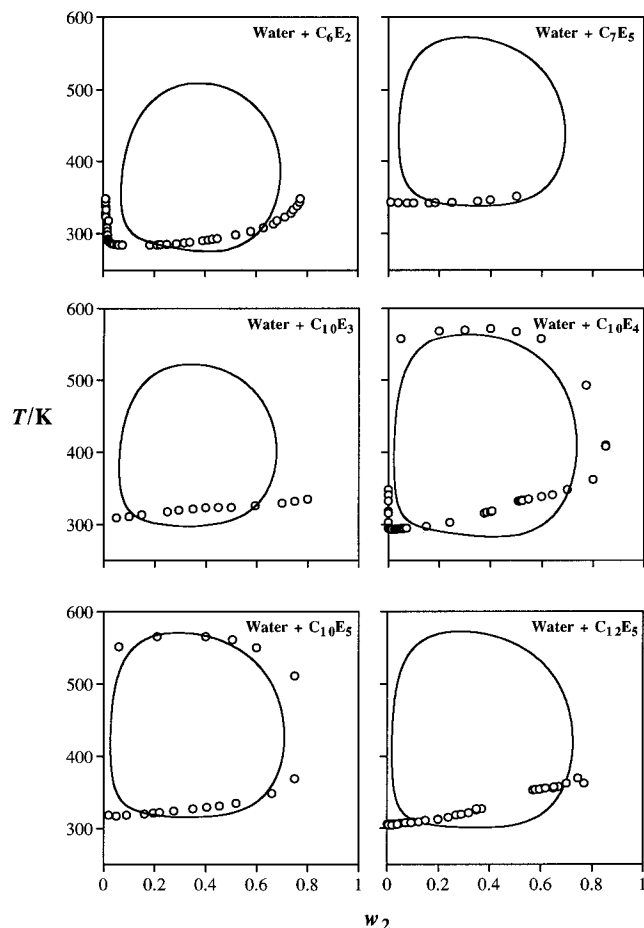


Figure 2. T_w , w being the weight fraction of surfactant, orthobaric curves for six aqueous mixtures: $\text{H}_2\text{O} + \text{C}_6\text{E}_2$, $\text{H}_2\text{O} + \text{C}_7\text{E}_5$, $\text{H}_2\text{O} + \text{C}_{10}\text{E}_3$, $\text{H}_2\text{O} + \text{C}_{10}\text{E}_4$, $\text{H}_2\text{O} + \text{C}_{10}\text{E}_5$, and $\text{H}_2\text{O} + \text{C}_{12}\text{E}_5$. The experimental compositions^{6,7,16,17,19,20} are represented as circles, and the calculated values are shown as solid curves.

$\epsilon_{012}^{\text{hb}}/k = 1874$ K is obtained. This value is again slightly different from that of $\epsilon_{012}^{\text{hb}}/k = 1986$ K used in paper I due to the small refinement to K_2 in the current work. As we studied the aqueous solutions of longer members of the C_iE_j series, it became apparent that it was possible to model the properties of the mixtures with these transferable values of $\epsilon_{12}^{\text{hb}}/k$ and $\epsilon_{012}^{\text{hb}}/k$ but that ϵ_{12} had to be adjusted in each case. This is not surprising considering the level of approximation of our theory and the considerable complexity of the micellar aggregates involved. The unlike integrated mean-field energy ϵ_{12} is therefore treated as the only adjustable parameter and its value optimized by fitting to the LCST of liquid–liquid phase equilibria of each particular water + C_iE_j system. In a sense, any difference in the intermolecular parameters of the members of the series is incorporated into ϵ_{12} in an average fashion. By using the optimized ϵ_{12} parameter, the region of liquid–liquid immiscibility for a large number of water + C_iE_j mixtures is successfully described by our theory, with an otherwise transferable set of parameters.

The experimental^{6,7,16,17,19,20} and predicted orthobaric cloud curves of liquid–liquid immiscibility for six of these systems are presented in Figure 2. The particular mixtures shown (for which there is a reasonable amount of experimental data available) with optimized unlike mean-field energy parameters are $\text{H}_2\text{O} + \text{C}_6\text{E}_2$ ($\epsilon_{12}/k = 3304$ K), $\text{H}_2\text{O} + \text{C}_7\text{E}_5$ ($\epsilon_{12}/k = 3023$ K), $\text{H}_2\text{O} + \text{C}_{10}\text{E}_3$ ($\epsilon_{12}/k = 3336$ K), $\text{H}_2\text{O} + \text{C}_{10}\text{E}_4$ (ϵ_{12}/k

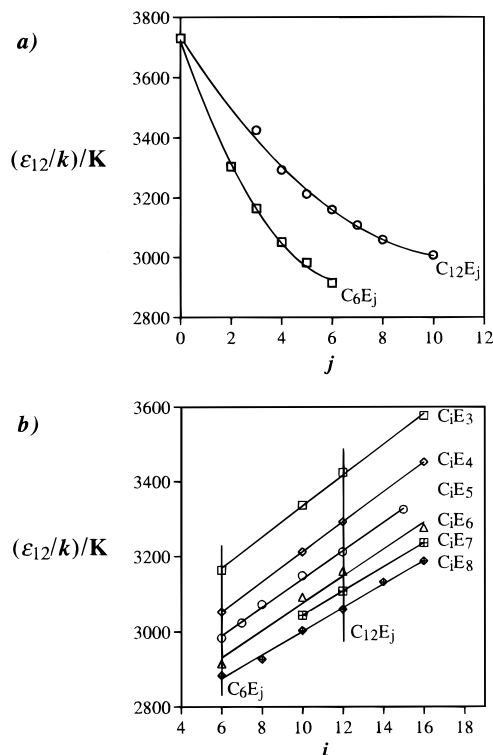


Figure 3. Dependence of the unlike integrated mean-field energy obtained from fits to particular water + C_iE_j mixtures for different numbers of oxyethylene groups and lengths of the alkyl residue in the surfactant molecule.

$= 3212$ K), $\text{H}_2\text{O} + \text{C}_{10}\text{E}_5$ ($\epsilon_{12}/k = 3148$ K), and $\text{H}_2\text{O} + \text{C}_{12}\text{E}_5$ ($\epsilon_{12}/k = 3212$ K). In all cases our theory gives a good description of the liquid–liquid immiscibility, the shape and position of the closed loops being in good overall agreement with the experimental curves. Considering that ϵ_{12} is optimized by fitting to the experimental LCSTs only, the predicted values of the UCSTs are in excellent agreement with the experimental points for the two systems for which experimental UCSTs are available ($\text{H}_2\text{O} + \text{C}_{10}\text{E}_4$ and $\text{H}_2\text{O} + \text{C}_{10}\text{E}_5$). Liquid crystalline (LC) phases have been observed experimentally in some of the mixtures shown in Figure 2, generally at low temperatures and high surfactant concentrations (e.g., see ref 7). Due to the inability of the theory in its present form to describe this type of phenomenon, the LC phases have been omitted.

A large number of $\text{H}_2\text{O} + \text{C}_i\text{E}_j$ mixtures are studied, and the unlike mean-field energy parameter ϵ_{12} is optimized to reproduce the LCST of the liquid–liquid immiscibility for each particular system as described earlier. The dependence of ϵ_{12} on the number of ethoxy groups j and the length of the alkyl residue i of the C_iE_j molecules is represented in Figure 3 for selected systems. It is interesting to see how the value of ϵ_{12} changes with the number of ethoxy groups for fixed values of i : the dependence is found to be well represented by a quadratic function of j for fixed values of i (in this case we show the results for $i = 6$ and $i = 12$). The specific dependence of ϵ_{12} is found to be even simpler with respect to i for a fixed value of j : the results shown in Figure 3b indicate that a simple linear relationship can be used to accurately describe the relation between ϵ_{12} and i . We have chosen the C_6E_j and C_{12}E_j series in order to obtain an analytical relation for the dependence of ϵ_{12} on i and j ; these systems have a sufficiently different chain length to enable an accurate interpolation/extrapolation for a wide number of C_iE_j systems. A linear least-squares fit of a quadratic polynomial in j to the values of ϵ_{12} given in Figure

Table 1. Predicted Critical Points for Water + C_iE_j Systems Using the Unlike Integrated Mean-Field Energy Obtained with Eq 15

	LCST/K										
	E ₁	E ₂	E ₃	E ₄	E ₅	E ₆	E ₇	E ₈	E ₉	E ₁₀	
C ₄	318 ^a 322 ^b		393 ^b	375 ^b	373 ^b	388 ^b	425 ^b				
C ₅		307 ^a 327 ^b	344 ^b	346 ^b	352 ^b	373 ^b	406 ^b	487 ^b			
C ₆		273 ^a 284 ^b	317 ^a	335 ^a	348 ^a	355 ^a	356 ^b	388 ^b	443 ^b		
C ₇				340 ^a							
C ₈			289 ^b 281 ^a	312 ^b 314 ^a	327 ^b 334 ^a	346 ^b 347 ^a	373 ^b 369 ^a	418 ^b 369 ^a			
C ₉				299 ^b	319 ^b	338 ^b	362 ^b	396 ^b	459 ^b		
C ₁₀				290 ^b	310 ^b	331 ^b	352 ^b	379 ^b	421 ^b	438 ^b	
C ₁₁			<273 ^a	293 ^a	319 ^a	334 ^a	349 ^a	358 ^a			
C ₁₂				289 ^b	308 ^b	325 ^b	343 ^b	366 ^b	392 ^b	396 ^b	
C ₁₃				284 ^b	307 ^b	323 ^b	337 ^b	354 ^b	371 ^b	364 ^b	
C ₁₄			<273 ^a	277 ^a	305 ^a	324 ^a	339 ^a	351 ^a			
C ₁₅				284 ^b	305 ^b	321 ^b	332 ^b	342 ^b	353 ^b	338 ^b	
C ₁₆				288 ^b	308 ^b	321 ^b	328 ^b	331 ^b	335 ^b		
C ₁₇			293 ^a			314 ^a	331 ^a	344 ^a			
				290 ^b	311 ^b	321 ^b	324 ^b	323 ^b	320 ^b		
			254 ^b	296 ^b	317 ^b	323 ^b	322 ^b	317 ^b			
			293 ^a	293 ^a		308 ^a	326 ^a	339 ^a			
			264 ^b	304 ^b	322 ^b	328 ^b	321 ^b	308 ^b			
			271 ^b	315 ^b	334 ^b	332 ^b	320 ^b	302 ^b			

^a Experimental values. ^b Predicted values.

3a for the C_6E_j and $C_{12}E_j$ systems results in the following expressions:

$$\epsilon_{12}(6, j) = 18.16j^2 - 242.9j + 3729 \quad (13)$$

$$\epsilon_{12}(12, j) = 5.630j^2 - 128.7j + 3729 \quad (14)$$

where $\epsilon_{12}(6, j)$ and $\epsilon_{12}(12, j)$ are the expressions of ϵ_{12} for the C_6E_j and $C_{12}E_j$ series, respectively.

If we make the reasonable assumption (based on the results shown in Figure 3b) that there is a simple linear dependence of ϵ_{12} on i for a fixed j and that the lines must pass through the values for the C_6E_j and $C_{12}E_j$ systems, then we obtain the following general relationship for ϵ_{12} :

$$\begin{aligned} \epsilon_{12}(i, j) &= \left(\frac{\epsilon_{12}(12, j) - \epsilon_{12}(6, j)}{6} \right) i \\ &+ \left(\epsilon_{12}(6, j) - \left(\frac{\epsilon_{12}(12, j) - \epsilon_{12}(6, j)}{6} \right) 6 \right) \\ &= \left(\frac{\epsilon_{12}(12, j) - \epsilon_{12}(6, j)}{6} \right) i + (2\epsilon_{12}(6, j) - \epsilon_{12}(12, j)) \\ &= (30.68j^2 - 357.1j + 3728) + i(-2.088j^2 \\ &+ 19.03j + 0.0705) \end{aligned} \quad (15)$$

The unlike mean-field parameter ϵ_{12} can thus be calculated with this expression for aqueous solutions of any member of the C_iE_j homologous series. This means that the phase equilibria of aqueous solutions for any member of the series can be predicted without further fitting; ϵ_{12} is the only adjustable parameter needed to complete the description of the intermolecular potentials.

Using this procedure, the orthobaric liquid–liquid phase equilibria of aqueous solutions of 140 members of the C_iE_j family have been analyzed. The results are summarized in Table 1, in the form of comparisons between the predicted and

experimental LCSTs. The existence of LCSTs has been reported for 30 $H_2O + C_iE_j$ systems (see ref 10 and references therein). Our theory predicts closed loops with corresponding LCSTs for 26 of these mixtures; in the other 4 cases, the predicted liquid–liquid immiscibility extends to lower temperatures and therefore an LCST cannot be observed. This is also the case for some systems represented in the bottom left- and right-hand corners of the table, the curves of liquid–liquid immiscibility reopening with decreasing temperature. When an LCST is successfully predicted and the result can be compared to experiment, the maximum discrepancy in the value of the LCST is 31 K ($H_2O + C_{16}E_8$), and in some cases the predicted and experimental values are within 1 K of each other (e.g., $H_2O + C_5E_2$ and C_6E_6). Finally, for certain systems represented in the top right-hand corner of the table, closed-loop behavior cannot be found theoretically; these cases differ from those mentioned earlier in that the liquid–liquid immiscibility disappears. The strength of the van der Waals unlike interaction calculated with eq 15 causes the two components of the mixture to become miscible at the pressure considered. It is gratifying to find, however, that there is no experimental evidence which indicates the existence of liquid–liquid immiscibility for those mixtures.

Note that with this simple expression for ϵ_{12} we can predict closed-loop behavior in aqueous solutions of molecules as different as C_4E_1 and $C_{17}E_8$ by applying the SAFT-HS theory with a unique set of parameters optimized for this family of compounds. Another advantage of our approach is that the study is not confined to systems for which there are experimental results. Important gaps in the experimental studies can be filled, and whole new series can be analyzed. This is clearly apparent from the table, where our predictions are not always complemented with experimental values, and therefore a few of the columns and rows are completely predictive.

Specific trends taken from Table 1 are shown in Figure 4. We show plots of experimental and predicted LCSTs against the number of carbons i on the alkyl residue of the surfactants, when the number of oxyethylene units j is fixed (corresponding to columns of Table 1). Note the accuracy of our predictions in most cases and how our results go beyond the experimental data. In the case of the C_iE_3 series the theory does not predict an LCST for $i = 8-14$; as discussed earlier the liquid–liquid immiscibility extends to lower temperatures, so that no LCST is found. This is in contrast with the experimental findings although the data for this series are inconclusive.

Another way of representing the adequacy of our theory is by plotting calculated LCSTs against the corresponding experimental values (see Figure 5a). The line represents perfect agreement between the experimental and predicted points. It is clear that most of our predictions fall very close to their experimental counterparts. The accuracy of our predictions compare well with an empirical correlation by Kahlweit et al.¹⁴ (see Figure 5b):

$$T_{\text{Kahlweit}}^{\text{LCST}} = (-1055 + 4282/i) + \frac{1448 - 5152/j}{1 + 1.2j} \quad (16)$$

where $T_{\text{Kahlweit}}^{\text{LCST}}$ is the temperature of the lower critical point (in degrees Celsius). The main difference between our predictions and those of Kahlweit¹⁴ is that our results are obtained from a well-defined theory while Kahlweit's come from a simple empirical relation which cannot be used to describe other regions of the phase diagram of the different mixtures.

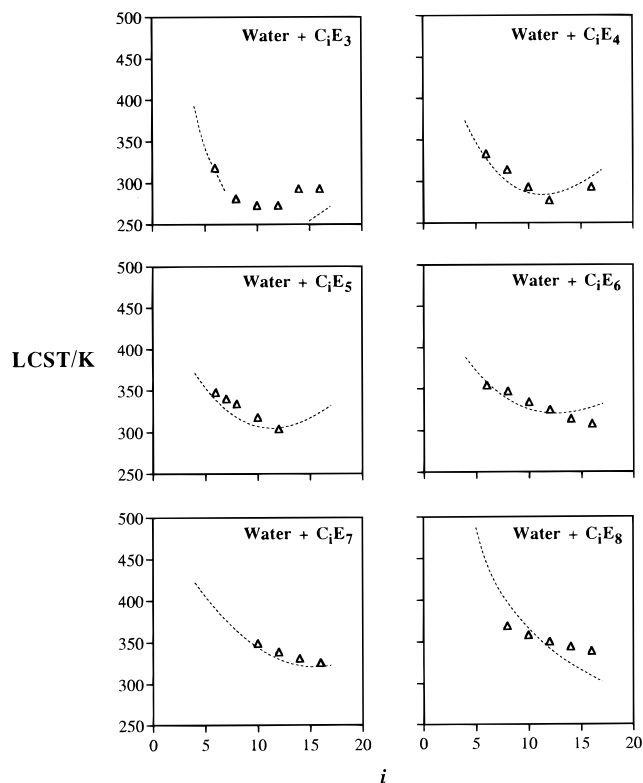


Figure 4. Comparison between experimental data points (ref 10 and references therein) and calculated curves (LCSTs) for water + C_iE_j mixtures, expressed as a function of the number of carbon atoms i in the alkyl chain of the surfactant. The integrated mean-field energy is obtained with eq 15 and is the only adjustable parameter used in the calculations.

Conclusions

A simple version of the SAFT approach (SAFT-HS) is used to describe the phase equilibria of water + alkyl polyoxyethylene mixtures. The properties of a large number of $H_2O + C_iE_j$ mixtures are obtained using a set of transferable parameters for the pure C_iE_j molecules and only one adjustable parameter for the mixtures, the others having been optimized by fitting to data for two systems. The formation of so-called closed loops is accurately described with our theory by allowing hydrogen bonding between the two components of the mixture. The hydrogen bonding between water and C_iE_j molecules is modeled through association between unlike bonding sites on the water and alkyl polyoxyethylene molecules. Furthermore, a single adjustable parameter in the mixture can be correlated to the structure of the different surfactant molecules represented by i and j . Using this analytical relationship, the theory is still capable of giving a good description of the phase behavior for aqueous solutions of the majority of the C_iE_j series. These predictions compare well with the available experimental data except for a handful of mixtures. One of the main advantages of our approach is the ability of our theory to describe any $H_2O + C_iE_j$ system on the basis of very limited experimental information from much simpler members of the homologous series.

The main motivation of the present work is in the transferable use of the parameters in the SAFT approach. We have already explored this feature in a recent paper,⁴⁶ in which the phase equilibria of water + n -alkane mixtures is predicted using transferable intermolecular parameters. In the present work we show that it is possible to use a similar approach and still describe the phase equilibria of the $H_2O + C_iE_j$ systems with

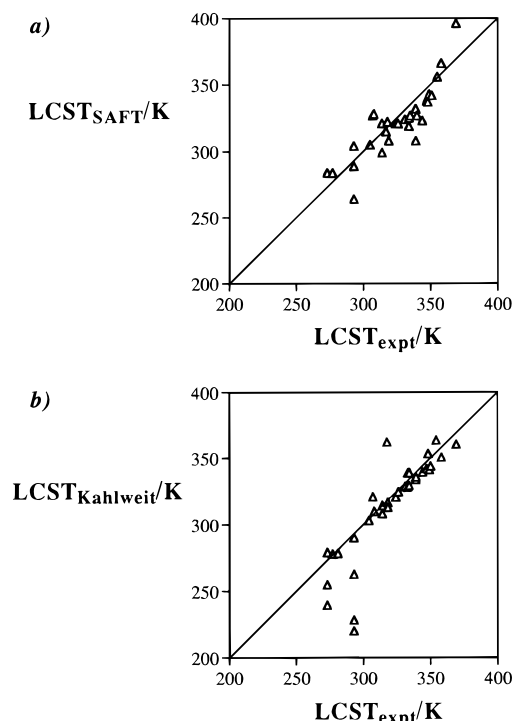


Figure 5. Correlation between experimental and calculated critical points (LCSTs) for water + C_iE_j mixtures: (a) calculated values from our present study, using the integrated mean-field energy obtained with eq 15; (b) critical points calculated with the empirical relationship of Kahlweit *et al.*¹⁴ (eq 16).

good accuracy. The additional complexity of our systems due to the presence of like and unlike hydrogen bonding in the mixtures does not compromise the adequacy of the SAFT-HS approach. The principle of transferability of intermolecular potentials is inherent to approaches like UNIQUAC.⁴⁹ However, the latter type of treatment leads to an overcorrection for nonrandomness in mixtures, and the theory has little predictive value. In their application of UNIFAC–UNIQUAC methods to the study of aqueous solutions of alkanes and nonionic surfactants, Knudsen and co-workers³¹ compare the performance of several of these models. Up to seven parameters are needed, some of which are temperature dependent, in order to achieve good agreement with experimental data at various thermodynamic states of the systems studied. In SAFT, however, the intermolecular potential parameters are temperature and pressure independent. With a unique set of intermolecular parameters fitted in a region of the phase diagram of a mixture, the theory can predict the full phase equilibria of the systems in good agreement with experiment. Furthermore, the theory is easily extended to the complete alkyl polyoxyethylene ether series with a minimum refitting of the parameters. The benefits of a strategy of transferable parameters in molecular simulations of phase equilibria are undeniable, and the research conducted in this area is too wide ranging to be quoted here. It is important, however, to mention some early work by Jorgensen⁵⁰ on transferable intermolecular potential functions for water, alkanes, alcohols, and other organic compounds, and more recent studies by Siepmann *et al.*⁵¹ and van Leeuwen and co-workers.^{52,53}

(49) Prausnitz, J. M.; Lichtenthaler, R. N.; Gomes de Azevedo, E. *Molecular Thermodynamics of Fluid Phase Equilibria*, 2nd ed.; Prentice Hall: Englewood Cliffs, NJ, 1986.

(50) Jorgensen, W. L. *J. Am. Chem. Soc.* **1981**, *103*, 335–340.

(51) Siepmann, J. I.; Karaborni, S.; Smit, B. *J. Am. Chem. Soc.* **1993**, *115*, 6454–6455.

Although not described here, it should be noted that our theory can be used to describe the full phase equilibria of a mixture, once the adequacy of the set of intermolecular parameters has been established. In our previous work (see paper I), we obtained the high-pressure phase equilibria of two aqueous systems (1-butanol and *n*-butoxyethanol) which were in excellent agreement with experimental data for the mixtures; the unlike parameters were optimized in a particular region of the phase diagrams. The treatment of the long-range dispersion forces at the rather crude level of van der Waals is justified by the satisfactory performance of the theory in predicting the phase equilibria of this type of mixture. This suggests that the most important nonideal contribution is due to association, which SAFT-HS treats within Wertheim's^{54,55} formalism. It is expected that the agreement with experiment would improve upon use of more sophisticated versions of SAFT, which treat dispersion forces in a more realistic manner.⁵⁶ Further improvement is expected to come from a more detailed description of the geometry of molecules. In its present form, SAFT, based

(52) van Leeuwen, M. E.; Smit, B. *J. Phys. Chem.* **1995**, *99*, 1831–1833.

(53) van Leeuwen, M. E. *Mol. Phys.* **1996**, *87*, 87–101.

(54) Wertheim, M. S. *J. Stat. Phys.* **1984**, *35*, 19–34, 35–47.

(55) Wertheim, M. S. *J. Stat. Phys.* **1986**, *42*, 459–476, 477–492.

(56) Gil-Villegas, A.; Galindo, A.; Whitehead, P. J.; Mills, S. J.; Jackson, G.; Burgess, A. N. *J. Chem. Phys.* **1997**, *106*, 4168–4186.

on the first-order perturbation theory of Wertheim, does not incorporate the precise geometry of the chain molecules. With regard to the phase equilibria of the systems studied here, the shape effects are expected to be less significant than the other thermodynamic factors. Small perturbations to the overall free energy due to the precise molecular shape are taken into account in a semiempirical sense through an effective chain length parameter, m . Naturally, the specific shape of the molecules will be important with regard to phenomena such as micelle formation, etc., where small free energy effects are crucial. In such cases, the Wertheim approach could be extended to second order⁵⁷ to refine the contributions due to the shape of the chain.

Acknowledgment. A.G. thanks Sheffield University and ICI for the award of a Roberts-Boucher Scholarship, and M.N.G.-L. thanks the European Union (Grant CII*-CT94-0132) and the EPSRC (ROPA Grant GR/K63436) for funding a research fellowship. We also acknowledge support from the Royal Society (Grant 574005.G501/1992) and from the Computational (Grant GR/H58810-C91) and ROPA (Grant GR/K34740) Initiatives of the EPSRC for computer hardware on which the calculations were performed.

JA9736525

(57) Muller, E. A.; Gubbins, K. E. *Mol. Phys.* **1993**, *80*, 957–976.